Chemical Physics Letters 739 (2020) 136984

Contents lists available at ScienceDirect

Chemical Physics Letters

journal homepage: www.elsevier.com/locate/cplett

Research paper

Decomposition of ammonia on $ZrB_2(0001)$

Weronika Walkosz[a,b,*], Kedar Manandhar[c], Michael Trenary[c], Peter Zapol[a]

[a] Materials Science Division, Argonne National Laboratory, 9700 S. Cass Ave., Argonne, IL 60439, United States
[b] Department of Physics, Lake Forest College, 555 N. Sheridan Rd., Lake Forest, IL 60045, United States
[c] Department of Chemistry, University of Illinois at Chicago, 845 W. Taylor Street, Chicago, IL 60607, United States

HIGHLIGHTS

- ZrB_2 is a substrate for the growth of Group-III nitrides using NH_3.
- NH_3 readily adsorbs onto the Zr-site of the ZrB_2 (0 0 0 1) surface.
- NH_3 dissociates to atomic N and H with relatively small activation barriers.
- The decomposition moieties (NH_2, NH, N and H) are very mobile on the surface.

ARTICLE INFO

Keywords:
ZrB_2
Group-III nitrides
GaN
NH_3 adsorption
DFT

ABSTRACT

Zirconium diboride has been recently identified as a promising substrate for the growth of Group-III nitride semiconductors using reactive vapors that include ammonia as the nitrogen source. Adsorption energies and dissociation pathways of NH_3 on the (0001) surface of ZrB_2 were investigated using density functional theory calculations. Our results indicate that NH_3 readily adsorbs onto the ZrB_2 surface terminated with Zr and decomposes to atomic N and H with relatively small activation barriers. The resulting atomic species are found to be mobile with the computed diffusion barriers between 0.11 and 0.78 eV.

1. Introduction

Group-III nitride semiconductors (GaN, InN, and AlN), have emerged as key materials for applications in visible and UV optoelectronics and in high-power and high-frequency electronics because of their tunable band gaps, high radiation hardness, and good thermal stability. Despite the remarkable progress in the commercialization of nitride-based devices, the lack of lattice-matched substrates for the growth of high quality nitride films still remains a technological challenge. A high defect density and biaxial strain due to the heteroepitaxial growth on foreign substrates such as α-Al_2O_3, SiC, Si, and ZnO, lead to grain boundaries, threading dislocations, stacking faults, and strong, built-in electrostatic fields, all limiting device performance and reliability. Therefore, the identification of lattice-matched substrates for epitaxial growth of group-III nitride films is highly desirable.

Kinoshita *et al.* have reported the synthesis of electrically conductive single crystals of ZrB_2 and proposed their use as substrates for the epitaxial growth of GaN [1]. The crystal structure of ZrB_2 is simple hexagonal with the lattice constants a = 3.169 Å and c = 3.530 Å, the former being only 0.63% larger than that of wurtzite GaN (a = 3.189 Å) [2]. The thermal expansion coefficient of ZrB_2 along $[10\bar{1}0]$ on the basal plane is $5.9 \times 10^{-6}\,K^{-1}$, which is also very close to that of GaN ($5.6 \times 10^{-6}\,K^{-1}$). This outstanding structural and thermal match between the two materials has led to high quality GaN films grown on ZrB_2 substrates by pulsed laser deposition (PLD) [3]. Promising outcomes have also been reported for the films grown by molecular beam epitaxy (MBE) and metal organic chemical vapor deposition (MOCVD), the latter being commonly used for the production of device-quality nitride films [4,5]. However, in the case of MOCVD growth, a low temperature buffer layer was necessary to prevent the substrate's complete nitridation. In this technique, growth occurs via gas phase and surface chemical reactions involving gallium and nitrogen containing precursors, such as trimethyl gallium and ammonia, respectively. Surface decomposition and diffusion reactions are thought to govern the growth, but their characterization is still lacking. A detailed quantification and understanding of the kinetics of precursor decomposition on the $ZrB_2(0001)$ surface is important for the controlled growth of GaN on the ZrB_2 substrates by MOCVD. While most of the computational and experimental studies on ZrB_2 have focused on its bulk properties [6–20], several studies investigated the $ZrB_2(0001)$

* Corresponding author.
E-mail address: vwalkosz@lakeforest.edu (W. Walkosz).

https://doi.org/10.1016/j.cplett.2019.136984
Received 14 August 2019; Received in revised form 18 November 2019; Accepted 23 November 2019
Available online 28 November 2019
0009-2614/

surface. Computationally, structure and bonding features of the bare and oxygenated ZrB_2(0001) surface were investigated with density functional theory (DFT) [21–23]. Experimentally, the ZrB_2(0001) surface subjected to thermal cleaning up to 1000 °C in vacuum as well as to treatment in HF aqueous solution was studied with X-ray photoelectron spectroscopy (XPS), reflection high-energy electron diffraction (RHEED), and atomic force microscopy (AFM) [24]. Surface phonon dispersion of ZrB_2(0001) was measured with high-resolution electron energy loss spectroscopy (HREELS) [25,26]. Aizawa *et al.* also studied the adsorption of H_2, $^2H_2$, O_2 and CO on the ZrB_2(0001) surface using the same technique [27]. The oxidation of ZrB_2(0001) at high temperature was studied using reflection high-energy electron diffraction, Auger electron spectroscopy, HREELS, and XPS [28] as well as DFT [29]. The surface and interface energies of GaN(0001) on ZrB_2(0001) were calculated with DFT [30,31]. Recently, we reported a combined DFT, XPS, and reflection absorption infrared spectroscopy (RAIRS) study of the adsorption of hydrogen and ammonia onto the (0001) surface of ZrB_2 [32–34]. Our results have indicated that the surface reacts with H and also facilitates NH_3 dissociation. We also studied the dissociation of trimethylgallium on the ZrB_2(0001) surface using X-ray photoelectron spectroscopy and RAIRS [35]. In this work, we perform a detailed investigation of NH_3 adsorption and decomposition pathways on the Zr-terminated (0001) surface of ZrB_2 using DFT. We report adsorption geometries and energies, transition states, intermediates, and activation barriers for the elementary decomposition reactions. The results are discussed in the context of the MOVPE growth mechanism of GaN on ZrB_2 substrates, and provide the basis for chemical kinetic models for more controlled nitride growth. Kinetic models based on DFT parametrization were successfully used in the past for the prediction of structure, properties, and reactivity of various materials [36–38]. The rest of the paper is organized as follows. In the next section, we provide details of the computational methods used in this work. The results and the discussion of the adsorption geometries and energies as well as NH_3 decomposition barriers are presented in Sections 3 and 4. We conclude with a brief discussion and summary in Sections 5 and 6, respectively.

2. Computational details

The ab-initio density functional theory (DFT) calculations were performed using the projector augmented wave (PAW) method in the VASP implementation [39,40]. The exchange-correlation interaction was treated with the generalized gradient approximation in the parameterization of Perdew, Burke, and Ernzerhof (PBE). A cutoff energy of 400 eV and a (4×4×1) Monkhorst-Pack grid were used for geometry optimizations. We focused on the Zr-terminated (0001) surface as it has been shown to be more stable than the B-terminated surface [21] as expected for Group IV metals [41]. The surface calculations were performed with the optimized lattice parameters (a = 3.179 Å and c = 3.548 Å) using a symmetric slab with a (2×2) surface unit cell consisting of seven atomic layers of ZrB_2. The optimized lattice parameters are in good agreement with the experimental [2,42] and other theoretically calculated results [10,13,21]. The vacuum layer size was ~17 Å in the direction normal to the surface. Only one side of the slab was used for adatom adsorption. Activation and diffusion barriers were calculated using the climbing image nudged elastic band method [43]. The adsorbate binding energies (*BE*) were calculated using the relation

$$BE = E_{surf+adsorb} - E_{surf} - E_{adsorb}$$

where $E_{surf+adsorb}$ is the total energy of the surface with the adsorbed species, E_{surf} is the total energy of the bare (relaxed) surface, E_{adsorb} is the total energy of gas phase NH_3, NH_2, NH, H, or N. The latter were calculated by placing the molecules in asymmetric (10×11×12 Å) cells. A negative value of *BE* implies an energetically favored adsorption process.

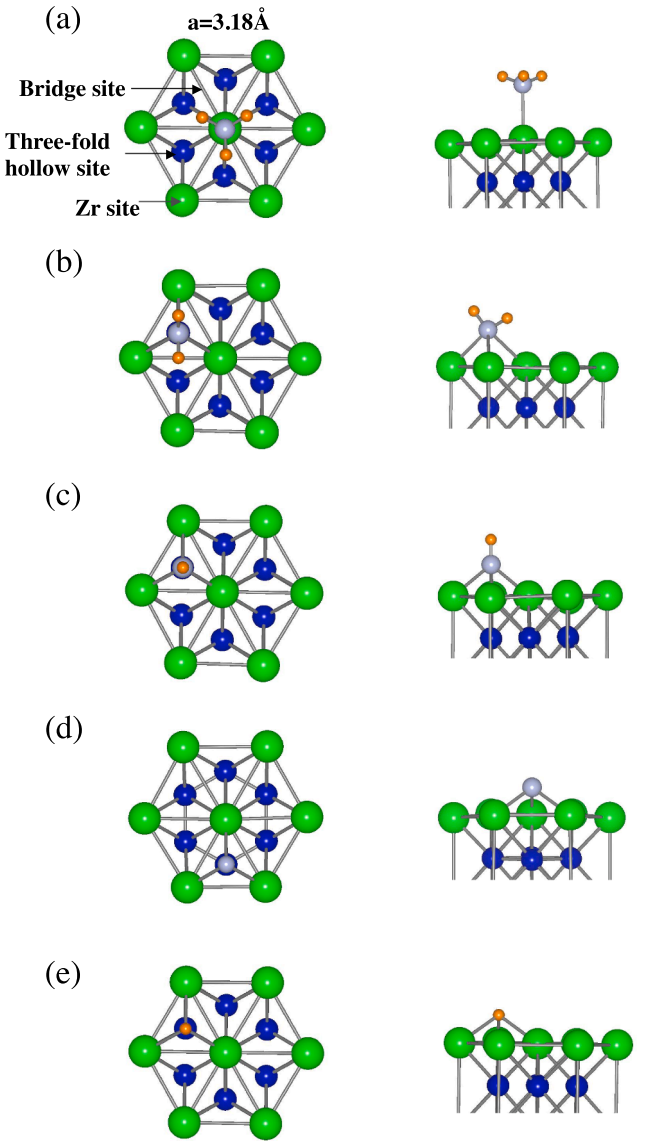

Fig. 1. Side (first column) and top (second column) views of the Zr-terminated (0001) surface of ZrB_2 with the adsorbed (a) NH_3 (b) NH_2 (c) NH (d) N (e) H in a (2×2) surface unit cell. Zr, B, N, and H atoms represented by green, grey, and orange spheres, respectively. (For interpretation of the references to color in this figure legend, the reader is referred to the web version of this article.)

3. Adsorption sites and energies

Geometry optimizations have been performed for NH_3, NH_2, NH, N, and H at different adsorption sites on the ZrB_2(0001) surface shown in Fig. 1. Table 1 lists the calculated *BE* for the adsorbates at their most favorable sites while the optimized structures are shown in Fig. 1. Ammonia adsorbs dissociatively on the Zr-terminated surface of ZrB_2, with the Zr site being a transition state site. The *BE* of NH_3 at this site is −0.95 eV and the N-Zr and N-H bond lengths are 2.38 Å and 1.03 Å, respectively. The three H-N-H angles are 109.21°. For comparison, the calculated intermolecular parameters of an isolated NH_3 molecule are 1.03 Å and 107.12°. We note here that we tested different rotational conformers for the initial positions of NH_3 on the diboride surface. As for NH_2, its most favorable site corresponds to the threefold hollow site between three surface Zr atoms with the *BE* of −4.30 eV. In this configuration, the NH_2 C_2-axis is perpendicular to ZrB_2(0001) and the H atoms point to the bridge and Zr sites. The calculated N−Zr bonds are 2.34, 2.42 and 2.42 Å, and the N−H bonds are 1.04 and 1.05 Å. The H−N−H angle is 102.66°. These parameters are similar to those of the

Table 1
Calculated binding energies (*BE*s) of different species on the Zr-terminated (0001) surface of ZrB_2.

Species	Site	BE (eV)	Bond lengths (Å)	H−N−H Angle (°)
NH_3	Zr	−0.95	N−Zr: 2.38; N−H: 1.03, 1.03, 1.03	109.21, 109.21, 109.21
NH_2	Hollow	−4.30	N−Zr: 2.34, 2.42, 2.42; N−H: 1.04, 1.05	102.66
NH	Hollow	−6.78	N−Zr: 2.22, 2.22, 2.22	~
N	Hollow	−2.72	N−Zr: 2.10, 2.10, 2.10	~
H	Hollow	−1.14	H−Zr: 2.15, 2.15, 2.15	~

gas phase NH_2 molecule (1.04 Å and 102.71°) calculated with DFT. Similarly to NH_2, the adsorption of NH is also the most favorable at the threefold hollow site with a *BE* of −6.78 eV and the three Zr−N and one N−H bonds of 2.22 Å and 1.03 Å in length, respectively. The calculated N−H bond of NH in gas phase was found to be 1.06 Å in length. Lastly, the adsorption configurations of N and H correspond to the threefold hollow sites with the *BE*s of −2.72 and −1.14 eV calculated with respect to atomic N and H, respectively. The N atom sits 2.96 Å above the subsurface B atom and it makes three bonds of 2.10 Å with the surrounding surface Zr atoms, whereas the H atom is 2.85 Å above the subsurface B and the Zr−H bonds are 2.15 Å in length. Comparing the species, the adsorption energies of NH_x (x = 1–3) become more negative when the number of H atoms decreases, while the molecules make shorter bonds with the surface Zr atoms. This indicates a stronger interaction of the dehydrogenated species with the surface. Similar trends were reported for NH_x (x = 1–3) on other surfaces [44–47].

4. Reaction pathways for decomposition of ammonia

Dehydrogenation reactions for the complete decomposition of NH_3 on the ZrB_2(0001) surface were studied in detail, with the product states of the reactions determined based on the stability of the NH_x species and the calculated activation barriers for each dehydration step. As stated in the previous section, the adsorption of ammonia onto the bare ZrB_2(0001) surface results in its decomposition to NH_2 and H at two non-neighboring hollow sites, thus reducing the electrostatic repulsion between the two moieties. The reaction is exothermic by 1.93 eV. In the second dissociation reaction, the adsorbed NH_2 molecule initially at the hollow site decomposes to NH and H at the two non-neighboring hollow sites. At the transition state geometry, the N−H bond is stretched to 1.33 Å. The barrier for this reaction is 0.23 eV and the process is exothermic by 1.52 eV. For NH dehydrogenation, the initial state corresponds to the NH molecule at the hollow site, while the final state consists of N and H at two non-neighboring hollow sites. At the transition state, the N−H bond is stretched to 1.42 Å. The activation barrier for this reaction is 1.37 eV and the process is exothermic by 0.17 eV.

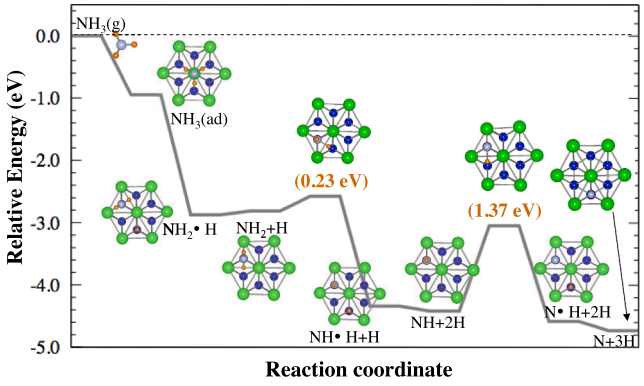

Fig. 2. Reaction pathway for ammonia decomposition by H abstraction on the ZrB_2(0001) surface. The (·) in the labels means that atoms are co-adsorbed in the same (2×2) surface unit cell, while (+) refers to the co-adsorption at large separation (without lateral interactions).

5. Discussion

To compare the reaction energies of the dehydrogenation steps discussed above, we referenced their adsorption energies to the NH_3 molecule in the gas phase. Fig. 2 shows the calculated reaction pathway for the complete decomposition of NH_3 at T = 0 K. In each step, the initial state is an NH_{3-x} (x = 0–2) species and x adsorbed H atoms without lateral interactions, while the final state corresponds to the NH_{3-x-1} species and one H atom co-adsorbed on the same (2×2) surface unit cell and x adsorbed H atoms at large separation. The pathway shows that the first two dehydrogenation steps, namely NH_3 and NH_2 decompositions to yield NH and H, are both kinetically and thermodynamically facile as their barriers are small and they are exothermic. Further decomposition to N and H has a significantly larger barrier (1.37 eV) and can be assumed to be the rate limiting step in the complete decomposition of NH_3 on ZrB_2(0001). However, the reaction is exothermic, thus favorable from the thermodynamic considerations. In fact, the whole decomposition process is thermodynamically favorable and there is no apparent barrier. Moreover, we find that the resulting moieties are fairly mobile, thus no significant energy needed to overcome decomposition barriers is expected to be lost due to their surface diffusion. The calculated barriers for NH_2, NH, N, and H migration between their stable sites are 0.11, 0.46, 0.78, and 0.27 eV respectively [32]. This implies that the complete decomposition of NH_3 to atomic N and H should ensue, especially at higher temperatures required for the MOCVD growth of Group-III nitrides. Although N deposition through NH_3 decomposition on ZrB_2 (0001) is a vital step in the nitride growth, previous work has shown that at high temperatures the surface becomes nitrided. The control of this process is a key to the growth of high-quality nitride films.

The prediction of complete dissociation of NH_3 on ZrB_2(0001) was verified by our recent XPS and RAIRS experiments for temperatures of 300 K and above [34]. However, the measurements have indicated that hydrogen-bonded clusters with the same structure as solid ammonia are formed on the diboride surface at lower temperatures. In this work, only one molecule per (2×2) surface unit cell was studied, thus no hydrogen bonding interactions were allowed. A deeper understanding of the atomic structures of the diboride surface in the ammonia environment will naturally require chemical kinetic models based on the ab initio calculations presented in this paper, incorporating more NH_3 molecules and using larger surface unit cells.

6. Conclusions

Density functional theory calculations have been performed for the adsorption and decomposition of NH_3 on the Zr-terminated (0001) surface of ZrB_2. We have predicted the adsorption sites, geometries, as well as the relative stabilities of the adsorbed ammonia and its dehydrogenated species. Our calculations show NH_3 readily adsorbs onto the Zr-site of the diboride surface and it dissociates to atomic N and H with relatively small activation barriers. The largest activation barrier corresponds to the NH decomposition. The complete dissociation of NH_3 was found to be exothermic, thus favorable from the thermodynamic considerations. Moreover, the resulting decomposition moieties were shown to be very mobile on the diboride surface.

CRediT authorship contribution statement

Weronika Walkosz: Conceptualization, Investigation, Writing - original draft. **Kedar Manandhar:** Conceptualization, Writing - review & editing. **Michael Trenary:** Conceptualization, Funding acquisition, Writing - review & editing. **Peter Zapol:** Conceptualization, Funding acquisition, Writing - review & editing, Supervision.

Declaration of Competing Interest

The authors declare that they have no known competing financial interests or personal relationships that could have appeared to influence the work reported in this paper.

Acknowledgements

This work was supported by the U. S. Department of Energy, Office of Science, Office of Basic Energy Sciences-Division of Materials Sciences and Engineering under Contract No. DE-AC02-06CH11357. M.T. acknowledges partial support from the National Science Foundation under grant CHE-1800236. We acknowledge grants of computer time from ANL Computing Resource Center (LCRC), ANL Center of Nanoscale materials (CNM), and the National Energy Research Scientific Computing Center (NERSC).

References

[1] H. Kinoshita, S. Otani, S. Kamiyama, et al., Zirconium diboride (0001) as an electrically conductive lattice-matched substrate for gallium nitride, Jpn. J. Appl. Phys. 40 (12A) (2001) L1280–L1282.
[2] Powder diffraction file, Joint Committee of Powder Diffraction Standard (JCPDS) No. 34–423.
[3] Yuji Kawaguchi, Atsushi Kobayashi, Jitsuo Ohta, Hiroshi Fujioka, Characteristics of GaN/ZrB_2 heterointerfaces prepared by pulsed laser deposition, Jpn. J. Appl. Phys. 45 (9A) (2006) 6893–6896, https://doi.org/10.1143/JJAP.45.6893.
[4] J. Suda, H. Matsunami, Heteroepitaxial growth of group-III nitrides on lattice-matched metal boride ZrB_2 (0001) by molecular beam epitaxy, J. Cryst. Growth 237 (2002) 1114–1117.
[5] Y. Tomida, S. Nitta, S. Kamiyama, et al., Growth of GaN on ZrB_2 substrate by metal-organic vapor phase epitaxy, Appl. Surf. Sci. 216 (1–4) (2003) 502–507.
[6] G. Fuchs, S.L. Drechsler, K.H. Muller, et al., A comparative study of MgB_2 and other diborides, J. Low Temp. Phys. 131 (5–6) (2003) 1159–1163.
[7] X.B. Wang, D.C. Tian, L.L. Wang, The electronic-structure and chemical-stability of the AlB_2-type transition-metal diborides, J. Phys.-Condens. Mater. 6 (46) (1994) 10185–10192.
[8] W.G. Fahrenholtz, G.E. Hilmas, I.G. Talmy, J.A. Zaykoski, Refractory diborides of zirconium and hafnium, J. Am. Ceram. Soc. 90 (5) (2007) 1347–1364.
[9] P. Vajeeston, P. Ravindran, C. Ravi, R. Asokamani, Electronic structure, bonding, and ground-state properties of AlB_2-type transition-metal diborides, Phys. Rev. B 63 (4) (2001) 045115.
[10] H.Z. Fu, Y. Lu, W.F. Liu, T. Gao, Pressure effects on elastic and thermodynamic properties of ZrB_2, J. Mater. Sci. 44 (20) (2009) 5618–5626.
[11] L. Huerta, A. Duran, R. Falconi, M. Flores, R. Escamilla, Comparative study of the core level photoemission of the ZrB_2 and ZrB_{12}, Physica C 470 (9–10) (2010) 456–460.
[12] M.G. Zhang, H. Wang, H.B. Wang, X.X. Zhang, T. Iitaka, Y.M. Ma, First-principles prediction on the high-pressure structures of transition metal diborides (TMB_2, TM = Sc, Ti, Y, Zr), Inorg. Chem. 49 (15) (2010) 6859–6864.
[13] H. Li, L.T. Zhang, Q.F. Zeng, et al., Crystal structure and elastic properties of ZrB compared with ZrB_2: a first-principles study, Comp. Mater. Sci. 49 (4) (2010) 814–819.
[14] S.C. Middleburgh, D.C. Parfitt, P.R. Blair, R.W. Grimes, Atomic scale modeling of point defects in zirconium diboride, J. Am. Ceram. Soc. 94 (7) (2011) 2225–2229.
[15] R. Kumar, M.C. Mishra, B.K. Sharma, et al., Electronic structure and elastic properties of TiB_2 and ZrB_2, Comp. Mater. Sci. 61 (2012) 150–157.
[16] J.W. Lawson, M.S. Daw, C.W. Bauschlicher, Lattice thermal conductivity of ultra high temperature ceramics ZrB_2 and HfB_2 from atomistic simulations, J. Appl. Phys. 110 (8) (2011) 083507.
[17] N.L. Okamoto, M. Kusakari, K. Tanaka, H. Inui, M. Yamaguchi, S. Otani, Temperature dependence of thermal expansion and elastic constants of single crystals of ZrB_2 and the suitability of ZrB_2 as a substrate for GaN film, J. Appl. Phys. 93 (1) (2003) 88–93.
[18] N.L. Okamoto, M. Kusakari, K. Tanaka, H. Inui, M. Yamaguchi, S. Otani, Mechanical and thermal properties of single crystals of ZrB_2, Defect Prop. Related Phenomena Intermetallic Alloys 753 (2003) 83–88.
[19] Zhi-Qian Chen, Yu-Si Peng, Meng Hu, Chun-Mei Li, Yan-Ting Luo, Elasticity, hardness, and thermal properties of ZrB_n(n = 1, 2, 12), Ceram. Int. 42 (6) (2016) 6624–6631, https://doi.org/10.1016/j.ceramint.2015.12.175.
[20] B.Z.W. Wang, W.D. Li, Mechanics lattice dynamics, and chemical bonding in ZrB_2 and ZrB_{12} from first-principles calculations, Sci. Adv. Mater. 5 (12) (2013) 1916–1921.
[21] X.H. Zhang, X.G. Luo, J.P. Li, J.C. Han, W.B. Han, C.Q. Hong, Structure and bonding features of ZrB_2 (0001) surface, Comp. Mater. Sci. 46 (1) (2009) 1–6.
[22] C.L.H.J. Cheng, Q.G. Fu, Initial oxidation of ZrB_2 (0 0 0 1) from first-principles calculations, Comp. Mater. Sci. 153 (2018) 282–287.
[23] W. Sun, J. Liu, H. Xiang, Y. Zhou, A Theoretical investigation on the anisotropic surface stability and oxygen adsorption behavior of ZrB_2, J. Am. Ceram. Soc. 99 (12) (2016) 4113–4120.
[24] R. Armitage, J. Suda, T. Kimoto, Characterization of ZrB_2 (0001) surface prepared by ex situ HF solution treatment toward applications as a substrate for GaN growth, Surf. Sci. 600 (7) (2006) 1439–1449.
[25] T. Aizawa, W. Hayami, S. Otani, Surface phonon dispersion of ZrB_2 (0001) and NbB_2 (0001), Phys. Rev. B 65 (2) (2002) 024303.
[26] T. Aizawa, S. Suehara, S. Hishita, S. Otani, Surface phonon dispersion of ZrB_2(0001) root 3 x root 3-B, J. Phys.-Condens. Mater. 20 (26) (2008) 265006.
[27] T. Aizawa, W. Hayami, S. Otani, Adsorption of H-2, H-2(2), O-2, and CO on ZrB (0001), J. Chem. Phys. 117 (24) (2002) 11310–11314.
[28] T. Aizawa, S. Hishita, S. Otani, The 2 x 2 oxidized layer on ZrB_2(0001), Appl. Surf. Sci. 256 (4) (2009) 1120–1123.
[29] H.K. Wang, X. Zhang, X.M. Qiu, Adaptive smoothed molecular dynamics for multiscale modeling, Comp. Mater. Sci. 46 (3) (2009) 713–715.
[30] J.I. Iwata, K. Shiraishi, A. Oshiyama, First-principle study on GaN epitaxy on lattice-matched ZrB_2 substrates, Appl. Phys. Lett. 83 (13) (2003) 2560–2562.
[31] P.-L. Liu, A.V.G. Chizmeshya, J. Kouvetakis, I.S.T. Tsong, First-principles studies of GaN(0001) heteroepitaxy on ZrB_2 (0001), Phys. Rev. B 72 (24) (2005) 245335.
[32] W. Walkosz, K. Manandhar, M. Trenary, S. Otani, P. Zapol, Dissociative adsorption of hydrogen on the ZrB_2 (0001) surface, Surf. Sci. 606 (23–24) (2012) 1808–1814.
[33] K. Manandhar, W. Walkosz, M. Trenary, S. Otani, P. Zapol, Dissociative adsorption of ammonia on the ZrB_2 (0001) surface, Surf. Sci. 615 (2013) 110–118.
[34] K. Manandhar, W. Walkosz, Y. Ren, S. Otani, P. Zapol, M. Trenary, Structure and reactivity of molecularly adsorbed ammonia on the ZrB_2 (0001) surface, J. Phys. Chem. C 118 (50) (2014) 29260–29269.
[35] K. Manandhar, M. Trenary, S. Otani, P. Zapol, Dissociation of trimethylgallium on the ZrB_2 (0001) surface, J. Vac. Sci. Technol., A 31 (6) (2013) 061405.
[36] J.K. Norskov, T. Bligaard, J. Rossmeisl, C.H. Christensen, Towards the computational design of solid catalysts, Nat. Chem. 1 (1) (2009) 37–46.
[37] D.A. Hansgen, D.G. Vlachos, J.G. Chen, Using first principles to predict bimetallic catalysts for the ammonia decomposition reaction, Nat. Chem. 2 (6) (2010) 484–489.
[38] D. Xu, P. Zapol, G.B. Stephenson, C. Thompson, Kinetic Monte Carlo simulations of GaN homoepitaxy on c- and m-plane surfaces, J. Chem. Phys. 146 (14) (2017) 144702.
[39] P.E. Blochl, Projector augmented-wave method, Phys. Rev. B 50 (24) (1994) 17953–17979.
[40] G. Kresse, J. Hafner, Abinitio molecular-dynamics for liquid-metals, Phys. Rev. B 47 (1) (1993) 558–561.
[41] K. Yamamoto, K. Kobayashi, H. Kawanowa, R. Souda, Difference in the outermost layer between TaB_2 (0001) and HfB2(0001), Phys. Rev. B 60 (23) (1999) 15617–15620.
[42] V.A. Epelbaum, M.A. Gurevich, On Zr-B phase diagram: Formation of ZrB_2 phase, Zh. Fiz. Khim. 32 (1958) 2274.
[43] G. Henkelman, B.P. Uberuaga, H. Jonsson, A climbing image nudged elastic band method for finding saddle points and minimum energy paths, J. Chem. Phys. 113 (22) (2000) 9901–9904.
[44] G. Novell-Leruth, A. Valcarcel, A. Clotet, J.M. Ricart, J. Perez-Ramirez, DFT characterization of adsorbed NH_x species on Pt(100) and Pt(111) surfaces, J. Phys. Chem. B 109 (38) (2005) 18061–18069.
[45] G. Novell-Leruth, A. Valcarcel, J. Perez-Ramirez, J.M. Ricart, Ammonia dehydrogenation over platinum-group metal surfaces. Structure, stability, and reactivity of adsorbed NH_x species, J. Phys. Chem. C 111 (2) (2007) 860–868.
[46] W. Walkosz, P. Zapol, G.B. Stephenson, A DFT study of reaction pathways of NH_3 decomposition on InN (0001) surface, J. Chem. Phys. 137 (5) (2012) 054708.
[47] W.Y. Huang, W.Z. Lai, D.Q. Xie, First-principles study of decomposition of NH_3 on Ir (100), Surf. Sci. 602 (6) (2008) 1288–1294.